

Zecca, A., Trainotti, E., Chiari, L., Bettega, M.H.F., d'A Sanchez, S., Varella, M.T. do N., Lima, M.A.P. and Brunger, M.J., 2012. Positron scattering from the cyclic ethers oxirane, 1,4-dioxane, and tetrahydropyran. Journal of Chemical Physics, 136, 124305



DOI: http://dx.doi.org/10.1063/1.3696378

# Positron scattering from the cyclic ethers oxirane, 1,4-dioxane, and tetrahydropyran

A. Zecca, E. Trainotti, L. Chiari, M. H. F. Bettega, S. d'A Sanchez et al.

Citation: J. Chem. Phys. **136**, 124305 (2012); doi: 10.1063/1.3696378
View online: http://dx.doi.org/10.1063/1.3696378
View Table of Contents: http://jcp.aip.org/resource/1/JCPSA6/v136/i12
Published by the American Institute of Physics.

# Positron scattering from the cyclic ethers oxirane, 1,4-dioxane, and tetrahydropyran

A. Zecca,[1] E. Trainotti,[1] L. Chiari,[1,2] M. H. F. Bettega,[3] S. d'A Sanchez,[3]
M. T. do N. Varella,[4] M. A. P. Lima,[5] and M. J. Brunger[2,6,a)]
[1]*Department of Physics, University of Trento, Povo, I-38123 Trento, Italy*
[2]*ARC Centre for Antimatter-Matter Studies, School of Chemical and Physical Sciences, Flinders University, GPO Box 2100, Adelaide, South Australia 5001, Australia*
[3]*Departamento de Física, Universidade Federal do Paraná, Caixa Postal 19044, 81531-990, Curitiba, Paraná, Brazil*
[4]*Instituto de Física, Universidade de São Paulo, Caixa Postal 66318, 05315-970, São Paulo, SP, Brazil*
[5]*Universidade Estadual de Campinas, Caixa Postal 6165, 13083-970, Campinas, São Paulo, Brazil*
[6]*Institute of Mathematical Sciences, University of Malaya, 50603 Kuala Lumpur, Malaysia*

(Received 24 January 2012; accepted 6 March 2012; published online 23 March 2012)

In this paper we report original measurements of total cross sections (TCSs) for positron scattering from the cyclic ethers oxirane ($C_2H_4O$), 1,4-dioxane ($C_4H_8O_2$), and tetrahydropyran ($C_5H_{10}O$). The present experiments focus on the low energy range from ~0.2 to 50 eV, with an energy resolution smaller than 300 meV. This study concludes our systematic investigation into TCSs for a class of organic compounds that can be thought of as sub-units or moieties to the nucleotides in living matter, and which as a consequence have become topical for scientists seeking to simulate particle tracks in matter. Note that as TCSs specify the mean free path between collisions in such simulations, they have enjoyed something of a recent renaissance in interest because of that application. For oxirane, we also report original Schwinger multichannel elastic integral cross section (ICS) calculations at the static and static plus polarisation levels, and with and without Born-closure that attempts to account for the permanent dipole moment of $C_2H_4O$. Those elastic ICSs are computed for the energy range 0.5–10 eV. To the best of our knowledge, there are no other experimental results or theoretical calculations against which we can compare the present positron TCSs. However, electron TCSs for oxirane (also known as ethylene oxide) and tetrahydropyran do currently exist in the literature and a comparison to them for each species will be presented. © *2012 American Institute of Physics*. [http://dx.doi.org/10.1063/1.3696378]

## I. INTRODUCTION

Particular interest has developed over the last decade, within the scientific community, to investigate the effect that low energy charged particles may cause when entering the human body,[1] specifically during medical therapies or diagnostic tests. While most medical devices initially start with very high-energy photons (e.g., x-rays), electrons or positrons (e.g., in positron emission tomography), this high-energy radiation quickly thermalises in the body through processes such as direct ionisation which in turn leads to the liberation of significant numbers of lower energy secondary electrons. Those secondary electrons may subsequently attach to the various components of DNA, causing important cell and tissue damage.[2,3] In addition, positron annihilation with electrons in those component molecules leads to a further form of ionisation and possible damage. These are just some of the reasons why it is interesting to study the interaction between low energy positrons and those molecules which can be considered as the "building blocks" of DNA.

As a consequence of the above, there are now several groups (see, e.g., Refs. 4–7 and references therein) using Monte Carlo simulation techniques in order to study particle tracks as those particles traverse through matter. Such studies ultimately aim to provide a nano-scale description of radiation damage in matter, and most if not all require a significant data base for the relevant atomic and molecular (ATMOP) processes that are occurring. Such an extensive data base should also be as accurate and reliable as possible. One component of such an ATMOP data base is the total cross section (TCS), which in essence is the probability that some type of collision will happen and is important as it defines the mean free path between collisions in such simulations.

We have therefore been undertaking a systematic study on measuring TCSs for positron scattering from a class of organic molecules, known generally as cyclic ethers, that might be considered as moieties to the nucleotides in living matter. Previous work includes scattering from tetrahydrofuran,[8] 3-hydroxy-tetrahydrofuran,[9] dihydropyran,[10] and $\alpha$-tetrahydrofurfuryl alcohol,[11] while in the present investigation we report new TCS results for positron scattering from oxirane or ethylene oxide ($C_2H_4O$), 1,4-dioxane ($C_4H_8O_2$), and tetrahydropyran ($C_5H_{10}O$), see Fig. 1. To assist us in better understanding our measured results for $C_2H_4O$, we have also undertaken Schwinger multichannel (SMC) calculations[12–14] at the static level (i.e., the

a)Electronic mail: Michael.Brunger@flinders.edu.au.

 

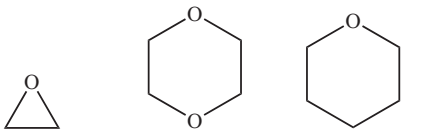


FIG. 1. Schematic diagrams representing the structures of the cyclic ethers: oxirane (ethylene oxide), 1,4-dioxane, and tetrahydropyran, as pertaining to this study.

Coulomb interaction between the incident positrons and the molecular electrons) and with inclusion of target polarisation. In both cases the Born-closure approximation[15] was also adopted, to try to account for the long-range character of the dipole potential of $C_2H_4O$. The results contained within this paper conclude our studies on the cyclic ethers. To the best of our knowledge, there are no other experimental or theoretical results for positron scattering from any of $C_2H_4O$, $C_4H_8O_2$, and $C_5H_{10}O$. The situation with respect to electron scattering is, however, a little better. In this regard, we mention the TCSs of Szmytkowski and Ptasińska-Denga[16] for electron scattering from tetrahydropyran in the 1–400 eV energy range. An independent atom model (IAM) based calculation result from Szmytkowski *et al.*[17] is also available for this system. Similarly, but now for ethylene oxide, the Gdańsk group have also reported electron–$C_2H_4O$ TCS measurements,[18] in this case for energies extending from 0.7–400 eV, and IAM theoretical results. Somewhat surprisingly, no electron–1,4-dioxane TCS appear to have been reported. We note that a comparison between the present positron TCSs and the corresponding electron TCSs[16–18] will be made later in this paper. In addition, here we also seek to investigate if there are any trends in the energy dependence of the positron total cross sections for all the cyclic ethers we have investigated, and if so can those trends be related to some of the more important physico-chemical properties (see Table I) of the species in question.[19–23]

In Sec. II we give a summary of our experimental apparatus and measurement techniques. Thereafter (Sec. III), details of our theoretical computations are provided. In Sec. IV, we report the present results and a discussion of those results, before drawing some conclusions from our investigation.

## II. EXPERIMENTAL DETAILS

The spectrometer at the University of Trento was developed by Zecca and collaborators and has been previously described.[25] We therefore do not repeat those details here, except for noting that a tungsten moderator of thickness 1 $\mu$m (Ref. 26) was employed in conjunction with a radioactive $^{22}$Na isotope (current activity ~1.6 mCi) and some electrostatic optics in order to produce the positron beam. Note that it is a standard practice in our laboratory, as a check for the validity of our techniques and procedures, to carry out preliminary validation measurements using targets for which positron scattering total cross sections might be considered to be well known. Such "well-characterised" systems might be drawn from the rare gases,[27,28] for example. We also employ molecular nitrogen[25] as an internal self-consistency check for apparatus performance.

TABLE I. Some of the important physico-chemical properties of the present cyclic ethers and also those from our previous investigations.[8–11] Note that (a) denotes the value pertaining to the first or global energy minimum conformer, while (b) denotes the value pertaining to the second or next highest energy conformer.

| Species | No. of electrons | First ionisation potential, IP (eV) | Positronium formation threshold, Ps (eV) | Dipole polarisability $\alpha$ (a.u.) | Dipole moment $\mu$ (D) |
|---|---|---|---|---|---|
| Ethylene oxide | 24 | 10.81[a] | 4.01 | 29.9[b] | 1.89[b] |
| Tetrahydrofuran[c] | 40 | 9.74 | 2.94 | 47.08 | 1.63 |
| 3-hydroxy-tetrahydrofuran[d] | 48 | 9.8 | 3.0 | (a) 50.68<br>(b) 50.98 | (a) 1.74<br>(b) 2.88 |
| 1,4-dioxane | 48 | 9.41[e] | 2.61 | 58.79[f] | ~0[f] |
| Di-hydropyran[g] | 46 | 8.6 | 1.8 | 64.92 | 1.38–1.48 |
| Tetrahydropyran | 48 | 9.26[h] | 2.46 | 66.13[i] | 1.58[j] |
| $\alpha$-tetrahydrofurfuryl alcohol[k] | 56 | 9.43 | 2.63 | 70.18 | ~2 |

[a]Reference 19.
[b]Reference 20.
[c]Reference 8.
[d]Reference 9.
[e]Reference 21.
[f]Reference 22.
[g]Reference 10.
[h]Reference 23.
[i]Reference 16.
[j]Reference 24.
[k]Reference 11.

The basis of all our linear transmission experiments is the Beer-Lambert law, as defined by

$$I_1 = I_0 \exp\left(\frac{-(P_1 - P_0)L\sigma}{kT}\right), \quad (1)$$

where $I_1$ is the transmitted positron count rate at pressure $P_1$, the target pressure being measured with the relevant species (ethylene oxide or 1,4-dioxane or tetrahydropyran) routed to the scattering cell, $k$ is Boltzmann's constant ($1.38 \times 10^{-23}$ JK$^{-1}$), and $T$ is the temperature of the species vapour (K), as accurately measured by using a calibrated platinum (PT100) resistance thermometer that is in excellent thermal contact with the scattering chamber. In our geometry, gas molecules thermalise with the scattering cell walls; therefore, the scattering chamber temperature can be considered a good approximation of the relevant gas temperature. Note that in this work the ethylene oxide sample holder was at room temperature, while 1,4-dioxane and tetrahydropyran were held at ~64 °C. Also in Eq. (1) $\sigma$ is the TCS of interest at a given incident positron energy; $I_0$ is the positron count rate at $P_0$, the pressure with the relevant species diverted into the vacuum chamber, i.e., away from the scattering cell; and $L$ is the length of the scattering region.

For a valid application of Eq. (1), several crucial precautions should be taken and care must be exercised during the measurements. Those considerations include minimising the double-scattering events and ensuring that the TCSs are independent of pressure. In addition, only high-purity ethylene

oxide (∼99.5%), 1,4-dioxane (∼99.8%), and tetrahydropyran (∼99%) target samples were used (Sigma-Aldrich). While ethylene oxide is a gas, 1,4-dioxane and tetrahydropyran are liquids but are sufficiently volatile to enable us to carry out our measurements. Further note that to minimise any possible impurities affecting our measurements, freeze-pump-thaw cycles were employed here for 1,4-dioxane and tetrahydropyran.

The geometrical length of the scattering region is 22.1 ± 0.1 mm, with apertures of 1.5 mm diameter at both the entrance and exit of the scattering cell. End effects were considered in all our studies, however, it is well known that such effects are minimised if both apertures have small and equal diameters such as in our case. As a consequence we believe their contribution to the uncertainty in the value of $L$ is likely to be less than 0.2%. In our application of Eq. (1), the value of $L$ used is always corrected to account for the path increase caused by the gyration of the positrons in the focussing axial magnetic field ($B$) present in the scattering region. For our work with $C_2H_4O$, $B \sim 11.4$ G leading to a correction of +5.7% on $L$, except for positron energies between 40.2–50.2 eV where $B \sim 4.8$ G and L increased by only ∼2.4%. In the case of 1,4-dioxane, $B \sim 11.2$ G leading to a correction of +5.5% on $L$, except now for positron energies between 30.2–50.2 eV where $B$ ∼4 G and $L$ increased by ∼2%. Finally, for tetrahydropyran, $B \sim 11.3$ G leading to a correction of +5.6% on $L$, except for positron energies between 30.2–50.2 eV where $B$ was again ∼4 G and $L$ increased by only ∼2%. From a consideration of the size of the entrance and exit apertures of our scattering cell, and their separation, the angular acceptance ($\Delta\theta$) of the Trento spectrometer is ≈4°, which compares favourably with that from the Detroit apparatus[29] ($\Delta\theta \approx 16°$). The gyration of the positrons can also potentially increase the angular resolution error compared to the no-field case.[30] This can also be corrected for, provided appropriate absolute elastic differential cross sections are available. Unfortunately, results for such differential cross sections (DCSs) (either theory or experiment) are currently unavailable for any of the three species of this work so that the TCSs we report here represent a lower bound on the exact values. Using some of the analytic formulae detailed in Kauppila *et al.*,[29] but for the typical conditions of our measurements, estimates of the present energy-dependent angular discrimination[31] can be obtained. We found they varied from ∼17.5° at 1 eV positron energy to ∼5.4° at 10 eV. With these data and appropriate elastic DCSs, at each energy, the present TCSs could in principle be corrected for the angular discrimination effect. A more quantitative discussion of the experimental angular discrimination and its effect on measured TCSs can be found in Sullivan *et al.*,[31] to whom the interested reader is referred for more details.

It is important in these experiments for the energy scale to be calibrated accurately. The zero for the energy, in the absence of any target gas, was determined in all our studies with a retarding potential analysis of the positron beam.[32] Measurements repeated during the last few years show a surprising stability in the energy zero (variance <0.05 eV) when using a tungsten moderator. We believe that the error in our energy scale calibration is ±0.1 eV. The same measurements allow us to evaluate an energy width smaller than 0.3 eV (FWHM) for our tungsten moderated positron beam.[26] It is also crucial to measure accurately the scattering cell pressure, which we achieve with a MKS 627B capacitance manometer that operated at a temperature of 45 °C. As the manometer temperature was different to that for the target gas of interest in the scattering cell, thermal transpiration corrections to the pressure readings are made using the model of Takaishi and Sensui.[33] For the $C_2H_4O$ measurements this correction was a maximum of +3.5% of the TCS, while for $C_4H_8O_2$ and $C_5H_{10}O$ the maximum correction was about −3%. One last caveat on the TCSs we report here should be noted. With an experimental energy resolution of ∼0.3 eV (FWHM), at positron energies below ∼0.5 eV the TCSs we report are actually a convolution over this energy resolution. In practice this physically implies that, when corrected for this effect, our lowest energy TCSs should be somewhat higher in magnitude than what is presented here. Note that the extent of this effect will depend on the energy dependence of the TCS, and is therefore expected to be species specific.

Finally, we note that the data collection and analysis codes were driven by software developed at the University of Trento, for application on a personal computer. The positron energy range of the present total cross section measurements was usually ∼0.2–50.2 eV, with the overall errors on our TCSs typically being within the range 5%–12%. All measurements were taken under stable positron beam conditions.

## III. THEORY DETAILS

To compute the integral cross sections (ICSs) for ethylene oxide we employed the Schwinger multichannel method (SMC) as implemented for positron-molecule collisions. The SMC method has been described in detail in Refs. 12–14 Here, we will only describe those aspects relevant to the present calculations.

The SMC method is an *ab initio* variational method to the scattering amplitude, whose final expression in the molecular reference (body) frame is

$$f(\vec{k}_f, \vec{k}_i) = -\frac{1}{2\pi} \sum_{m,n} \langle S_{\vec{k}_f} | V | \chi_m \rangle (d^{-1})_{mn} \langle \chi_n | V | S_{\vec{k}_i} \rangle, \tag{2}$$

where

$$d_{mn} = \langle \chi_m | A^{(+)} | \chi_n \rangle, \tag{3}$$

$$A^{(+)} = Q\hat{H}Q + PVP - VG_P^{(+)}V. \tag{4}$$

In the above equations, $|S_{\vec{k}_{i,f}}\rangle$ is a solution of the unperturbed Hamiltonian $H_0$ defined as the sum of the kinetic energy of the incoming positron and the target Hamiltonian ($T_{N+1} + H_N$). It is written as a product of a target state and a plane wave ($|\vec{k}\rangle \otimes |\Phi_i\rangle$). $V$ is the interaction potential between the incident positron and the electrons and nuclei of the molecular target; $\{|\chi_m\rangle\}$ is a set of $(N+1)$-particle functions (configuration state functions, CSFs). This set is used to expand the trial scattering wave function. $\hat{H} = E - H$ is the total energy of the collision minus the full Hamiltonian of the system, with $H = H_0 + V$. $P$ is a projection operator onto the open-channel space defined by the target eigenfunctions, and $G_P^{(+)}$

is the free-particle Green's function projected on the $P$-space. The projection operator onto the closed electronic channels of the target $Q$ is defined as $Q = (\mathbb{1} - P)$. The $Q$-space define the CSFs used in the description of polarisation effects (distortion of the electronic molecular cloud due to the presence of the incoming positron).

In the calculations carried out in the static (S) approximation, where polarisation effects are completely neglected, the direct space is constructed considering CSFs of the form,

$$|\chi_i\rangle = |\Phi_1\rangle \otimes |\varphi_i\rangle, \tag{5}$$

where $|\Phi_1\rangle$ is a $N$-electron Slater determinant of the target ground state obtained at the Hartree-Fock level and $|\varphi_i\rangle$ is a one particle function which represents the incoming positron. The set composed by the one particle functions are used as scattering orbitals.

In the calculations that take polarisation (P) effects into account the direct space is enlarged by considering CSFs from the $Q$ (closed-channel) space. These configurations are constructed as

$$|\chi_{ij}\rangle = |\Phi_i\rangle \otimes |\varphi_j\rangle, \tag{6}$$

where $|\chi_{ij}\rangle$ is a $N$-particle Slater determinant and is obtained by performing single (virtual) excitations from the occupied molecular (hole) orbitals to a set of unoccupied molecular (particle) orbitals. The $|\varphi_j\rangle$ is again a one particle function used as a scattering orbital. The choice of the particle and scattering orbitals will be discussed below.

Our calculations were performed in the static and in the static plus polarisation (S+P) approximations at the ground state equilibrium geometry of the molecule, as given in Ref. 34. The target was treated as a $C_{2v}$ molecule. The basis set employed in both bound state and scattering calculations for oxygen, carbon, and hydrogen are the same as used in our previous work on positron-formaldehyde collisions.[35] The particle and scattering orbitals were represented by the improved virtual orbitals (IVOs),[36] which were obtained by diagonalizing the Fock operator in the field of $N - 1$ electrons. In the present calculations we considered all the valence occupied orbitals as hole orbitals and considered excitations to the lower 45 IVOs to represent the particle orbitals. The scattering orbitals were represented by the occupied orbitals plus the 45 lower IVOs. We then obtained 6273 CSFs for $A_1$ symmetry, 5531 CSFs for $B_1$ symmetry, 6086 CSFs for $B_2$ symmetry, and 5349 CSFs for the $A_2$ symmetry.

Ethylene oxide possesses a permanent electric dipole moment. The calculated dipole moment of the target was 2.30 D, which is slightly higher than the experimental value of 1.89 D.[20] The SMC method uses square-integrable basis sets in the representation of the scattering wave function. However, these functions cannot account for the long-range dipole interaction. In order to capture the long-range character of the dipole potential in our calculations we employed the standard Born-closure (BC) scheme to the scattering amplitude.[15] In the present calculations we chose $\ell_{SMC} = 2$ from 0.5 to 4.0 eV and $\ell_{SMC} = 3$ from 4.5 to 10 eV. The values of $\ell_{SMC}$ were chosen in order to minimize the differences between the DCSs computed with the SMC method and with the Born-closure scheme above $\sim 30^\circ$.

Throughout the present paper we will adopt the following nomenclature. For the SMC calculations that include the BC scheme and are conducted at the static level we will denote by BC–S. Those same calculations that additionally include polarisation are denoted as BC–S+P. Similarly, the computations where the Born-closure scheme is ignored are denoted as SMC–S and SMC–S+P, respectively.

## IV. RESULTS AND DISCUSSION

In this section we begin by considering in turn the three cyclic ethers of the present study. Thereafter, we compare the TCSs for all the cyclic ethers investigated at the University of Trento, and see if their behaviour can in some way be related to some of their physico-chemical properties as listed in Table I.

### A. Ethylene oxide (oxirane)

In Table II and Fig. 2, we present the results of our positron–$C_2H_4O$ total cross section measurements. Note that the uncertainties listed in Table II and plotted in Fig. 2 are purely statistical and are at the one standard deviation level. Further note that the arrows in Fig. 2 indicate, respectively, the approximate thresholds for positronium formation (Ps) and the direct (first) ionisation potential (IP) in $C_2H_4O$. Both those values can also be found in Table I. In Fig. 2 we also plot the elastic ICS results from our BC–S, BC–S+P, SMC–S, and SMC–S+P level computations, which are now discussed and compared to our measured data in more detail below.

The important roles played in the positron–$C_2H_4O$ scattering dynamics, by the target dipole moment and dipole polarisability, are easily educed from Fig. 2. Specifically, the role of the dipole moment can be seen when we compare the results of our BC–S+P calculation with those from our SMC–S+P computation (or, equally well, the BC–S integral

TABLE II. Present TCSs ($\times 10^{-20}$ m$^2$) for positron scattering from oxirane (ethylene oxide). The errors given represent the statistical uncertainty component only of the overall error. See text for further details.

| Energy (eV) | TCS ($10^{-20}$ m$^2$) | TCS error ($10^{-20}$ m$^2$) ($\pm 1\sigma$) | Energy (eV) | TCS ($10^{-20}$ m$^2$) | TCS error ($10^{-20}$ m$^2$) ($\pm 1\sigma$) |
|---|---|---|---|---|---|
| 0.30 | 135.47 | 4.06 | 6.2 | 20.78 | 0.91 |
| 0.40 | 112.01 | 4.51 | 6.7 | 19.62 | 0.09 |
| 0.50 | 101.80 | 1.97 | 7.2 | 19.15 | 0.46 |
| 0.60 | 87.84 | 0.33 | 8.2 | 19.10 | 0.26 |
| 0.80 | 70.77 | 0.92 | 9.2 | 18.06 | 0.37 |
| 1.00 | 60.34 | 1.07 | 10.2 | 17.89 | 0.33 |
| 1.20 | 51.57 | 2.02 | 12.7 | 17.57 | 0.34 |
| 1.45 | 46.12 | 0.81 | 15.2 | 17.55 | 0.47 |
| 1.70 | 41.28 | 0.46 | 20.2 | 17.19 | 0.11 |
| 1.95 | 36.30 | 0.45 | 25.2 | 17.52 | 0.11 |
| 2.20 | 32.67 | 0.59 | 30.2 | 16.73 | 0.47 |
| 2.70 | 28.81 | 1.09 | 35.2 | 16.43 | 0.11 |
| 3.20 | 26.50 | 0.50 | 40.2 | 16.18 | 0.38 |
| 4.20 | 24.06 | 1.16 | 45.2 | 16.07 | 0.28 |
| 5.20 | 20.28 | 0.55 | 50.2 | 16.34 | 0.04 |

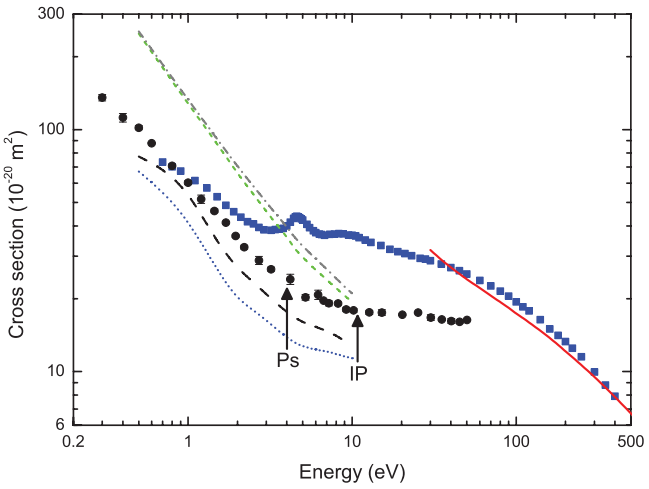


FIG. 2. TCSs ($\times 10^{-20}$ m$^2$) for positron scattering from ethylene oxide. The present data are denoted by (●). The positronium formation threshold and the first ionisation potential are indicated by arrows labelled "Ps" and "IP." The current computational ICS results are also shown: BC–S (– · –), BC–S+P (- - -), SMC–S (– –), and SMC–S+P ( · · · ). Also plotted are electron scattering TCSs from Szmytkowski *et al.*[18] (■) and their corresponding IAM theory results (——).

cross sections with the SMC–S integral cross sections). Similarly, the effect of the target polarisation can be seen when we compare our BC–S+P results with those from our BC–S calculation (or, equally well, our SMC–S+P ICSs with our SMC–S ICSs). In all cases the effect of incorporating polarisation and/or the dipole moment on the magnitude of the ICS is manifest, with the inclusion for the permanent dipole moment of $C_2H_4O$ apparently having the largest effect in this case. When we now compare our theoretical results to the present measured TCSs, we find generally quite good qualitative (energy dependence) accord between them. However, there are some significant differences in terms of the magnitude. Indeed, this comparison is reminiscent of what we previously found for positron scattering from both formaldehyde[35] and formic acid[37] and the major reasons for those discrepancies that we advanced in those earlier studies are also applicable here. Namely, it is well known[35] that the Born-closure approach can cause a quite significant overestimation of the elastic ICSs, which is in part why our (in principle) most accurate computation, the BC–S+P calculation, has elastic ICSs that are greater in magnitude than the measured TCSs. This situation is clearly unphysical. From an experimental perspective, the major cause of the discrepancy is most likely that the present TCSs have not been corrected for forward-angle scattering effects.[31] As Makochekanwa *et al.*[38] showed for $H_2O$ and HCOOH, which have dipole polarisabilities of significant magnitude and strong permanent dipole moments such as $C_2H_4O$, the correction (increase) in the TCSs, particularly at low incident positron energies, could be large and becoming even greater as you go to progressively lower energies. In principle we could use the present calculated elastic differential cross sections to correct for this effect, however given the level of agreement between theory and experiment for the integrated cross sections in Fig. 2 such a move would seem premature at this time.

To the best of our knowledge there are no other experimental or theoretical TCSs for positron scattering from ethylene oxide. However, in Fig. 2 we provide the only available electron–ethylene oxide TCS measurement from Szmytkowski *et al.*[18] and an independent atom model calculation result from that same group. Let us now look at the experimental positron results, where it is clear that as you go to lower positron energies the magnitude of the TCSs increases strongly (note the log-scale on the y axis). This magnitude is even more significant when one considers the following two factors. First, with an energy resolution ~0.3 eV, our lowest energy TCSs ($\lesssim$0.5 eV) are actually a convolution over this energy width. In practice, this implies that when the TCSs are corrected for this effect they will likely increase further in magnitude. Second, we reiterate that the data in Table II are not corrected for the imperfect forward angle discrimination of the spectrometer, which if implemented could see very large increases in the measured TCSs particularly at the lower energies.[38] The low-energy behaviour of the present positron–ethylene oxide total cross sections was not unexpected, as we have encountered similar trends in our previous work on polar biomolecules,[8–11,35,37,39–41] which we have ascribed to the strong dipole moments and significant dipole polarisabilities of those species. The current positron–$C_2H_4O$ TCS shows a largely monotonic decrease in value with increasing positron energy, until first the positronium channel and then the direct ionisation channel successively open. The opening of these channels is usually seen as a small "structure" or slope change in the measured TCSs, as is the case here. Note that such a change might be better appreciated in Fig. 5, where the same TCS is plotted with a different (expanded) energy scale. Finally, for energies above about 10 eV we note how "flat" or "constant" the present TCS for ethylene oxide appears to be. This "flat" appearance possibly suggests a relatively small contribution to the TCS from the positronium formation channel, with an ionisation channel contribution that might only be slightly larger.

Comparing now our positron TCSs and the measured electron TCSs of Szmytkowski *et al.*,[18] we find that in the common range of energy there is little similarity between them. Indeed, except at the very lowest energies, the electron TCSs are greater in magnitude compared to those of the positron scattering case. In addition, the electron data exhibits strong shape resonance phenomena whereas no such behaviour appears in the positron channel. However, the trend in the present positron-TCS suggests that by an energy of about 200–300 eV it will have converged to that for the electron-TCS. This we believe is physical, as the two most important phenomenological differences between the electron and positron scattering processes – exchange in the case of the incident electrons and positronium formation in the case of the incident positrons – both typically become small at incident projectile energies above 100 eV.

### B. 1,4-dioxane

In Table III and Fig. 3, we present the results of our positron–1,4-dioxane total cross section measurements. It

TABLE III. Present TCSs ($\times 10^{-20}$ m$^2$) for positron scattering from 1,4-dioxane. The errors given represent the statistical uncertainty component only of the overall error. See text for further details.

| Energy (eV) | TCS ($10^{-20}$ m$^2$) | TCS error ($10^{-20}$ m$^2$) ($\pm 1\sigma$) | Energy (eV) | TCS ($10^{-20}$ m$^2$) | TCS error ($10^{-20}$ m$^2$) ($\pm 1\sigma$) |
|---|---|---|---|---|---|
| 0.20 | 230.22 | 7.34 | 3.15 | 49.57 | 0.32 |
| 0.25 | 207.56 | 7.01 | 4.15 | 43.65 | 0.77 |
| 0.27 | 190.25 | 8.34 | 5.15 | 40.14 | 0.36 |
| 0.30 | 184.84 | 7.90 | 6.15 | 38.15 | 0.32 |
| 0.32 | 179.31 | 1.86 | 7.15 | 36.81 | 0.36 |
| 0.35 | 175.60 | 5.74 | 8.15 | 35.32 | 0.61 |
| 0.40 | 162.37 | 4.17 | 9.15 | 33.90 | 0.49 |
| 0.45 | 152.02 | 3.72 | 10.2 | 33.57 | 0.53 |
| 0.50 | 145.08 | 1.89 | 12.7 | 31.81 | 0.62 |
| 0.55 | 139.70 | 6.04 | 15.2 | 31.81 | 0.04 |
| 0.60 | 128.10 | 7.45 | 17.7 | 30.46 | 0.35 |
| 0.65 | 120.86 | 1.30 | 20.2 | 29.56 | 1.26 |
| 0.75 | 113.16 | 2.70 | 22.2 | 29.50 | 1.05 |
| 0.85 | 105.23 | 1.68 | 25.2 | 28.60 | 0.84 |
| 0.95 | 97.05 | 1.78 | 27.2 | 28.07 | 0.45 |
| 1.15 | 83.39 | 1.79 | 30.2 | 27.10 | 0.32 |
| 1.40 | 74.74 | 1.68 | 35.2 | 26.63 | 0.33 |
| 1.65 | 66.81 | 0.94 | 40.2 | 27.87 | 0.20 |
| 1.90 | 60.90 | 0.57 | 45.2 | 27.14 | 0.22 |
| 2.15 | 57.48 | 1.05 | 50.2 | 27.16 | 0.30 |
| 2.65 | 52.09 | 0.92 | | | |

should be clear from Fig. 3 that there are no other theoretical or experimental positron and electron TCS against which we can compare our results. The errors plotted in Fig. 3 (and listed in Table III) are again purely statistical and at the one standard deviation level.

Much of the description provided above for ethylene oxide is equally applicable to 1,4-dioxane. Namely, the TCS is strongly peaked in magnitude at lower positron energy and it decreases monotonically in magnitude with increasing positron energy until the opening of the positronium formation channel and then the direct (first) ionisation channel cause subtle changes in the energy dependence of the TCS in each case. Nonetheless it remains a largely featureless distribution. Again we have here (see Fig. 3) a hint for only a small positronium formation contribution to the TCS, possibly even smaller than in the ethylene oxide case. The low energy behaviour of 1,4-dioxane, which has a zero dipole moment (see Table I), is attributed to its significant dipole polarisability $\alpha \sim 59$ a.u. This value is essentially twice that of the dipole polarisability of ethylene oxide (see Table I), so that it is interesting to compare the TCSs for the two species at low energies. For instance, at 0.5 eV the TCS of 1,4-dioxane is $145.08 \times 10^{-20}$ m$^2$ while that for ethylene oxide is $101.80 \times 10^{-20}$ m$^2$, a ratio $\sim$1.43 which is actually fairly consistent at all the energies between 0.3–0.8 eV for the TCS of both species. Of course, this analysis is complicated as ethylene oxide also has a permanent dipole moment whereas 1,4-dioxane does not, while the number of effective scattering centres and the geometric dimensions in 1,4-dioxane are bigger than those of ethylene oxide. So while the relative behaviour of the low energy TCSs of these species might be reflected to some degree in the ratio of their dipole polarisabilities, the size of the two species and the permanent dipole moment of the ethylene oxide are also playing key roles in this comparison.

### C. Tetrahydropyran

For positron scattering from tetrahydropyran, we are able to compare to corresponding electron total cross section data from Szmytkowski and Ptasińska-Denga[16] and results from the independent atom model calculations of Szmytkowski *et al.*[17] All these results, both positron and electron, are shown in Fig. 4, with the present positron–$C_5H_{10}O$ TCSs also

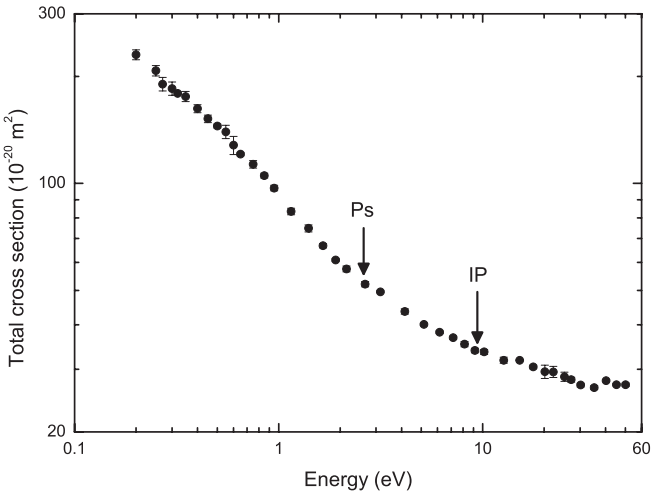


FIG. 3. TCSs ($\times 10^{-20}$ m$^2$) for positron scattering from 1,4-dioxane. The present data are denoted by (•). The positronium formation threshold and the first ionisation potential are indicated by arrows labelled "Ps" and "IP."

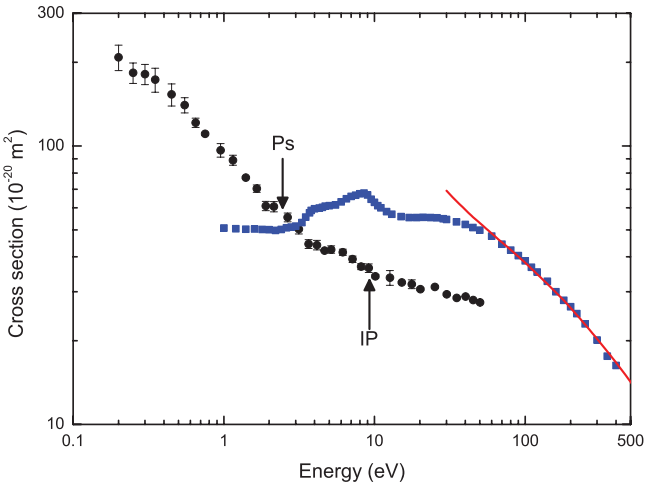


FIG. 4. TCSs ($\times 10^{-20}$ m$^2$) for positron scattering from tetrahydropyran. The present data are denoted by (•). The positronium formation threshold and the first ionisation potential are indicated by arrows labelled "Ps" and "IP." Also plotted are electron scattering TCSs from Szmytkowski and Ptasińska-Denga[16] (■) and their corresponding IAM theory results (——).[17]

TABLE IV. Present TCSs ($\times 10^{-20}$ m$^2$) for positron scattering from tetrahydropyran. The errors given represent the statistical uncertainty component only of the overall error. See text for further details.

| Energy (eV) | TCS ($10^{-20}$ m$^2$) | TCS error ($10^{-20}$ m$^2$) ($\pm 1\sigma$) | Energy (eV) | TCS ($10^{-20}$ m$^2$) | TCS error ($10^{-20}$ m$^2$) ($\pm 1\sigma$) |
|---|---|---|---|---|---|
| 0.20 | 208.51 | 21.89 | 4.65 | 42.15 | 0.12 |
| 0.25 | 183.35 | 15.53 | 5.15 | 42.49 | 1.31 |
| 0.30 | 181.42 | 15.16 | 6.15 | 41.57 | 1.05 |
| 0.35 | 173.23 | 17.10 | 7.15 | 39.25 | 1.04 |
| 0.45 | 153.26 | 13.85 | 8.15 | 36.90 | 0.91 |
| 0.55 | 140.37 | 8.71 | 9.15 | 36.46 | 1.29 |
| 0.65 | 121.27 | 4.63 | 10.2 | 34.06 | 0.44 |
| 0.75 | 110.60 | 1.39 | 12.7 | 33.66 | 2.03 |
| 0.95 | 96.67 | 5.47 | 15.2 | 32.37 | 0.28 |
| 1.15 | 89.01 | 3.74 | 17.7 | 31.92 | 1.14 |
| 1.40 | 77.08 | 0.62 | 20.2 | 30.64 | 0.37 |
| 1.65 | 70.35 | 2.12 | 25.2 | 31.17 | 0.31 |
| 1.90 | 60.98 | 2.31 | 30.2 | 29.35 | 0.32 |
| 2.15 | 60.63 | 2.59 | 35.2 | 28.49 | 0.31 |
| 2.65 | 55.48 | 2.01 | 40.2 | 28.82 | 0.07 |
| 3.15 | 50.31 | 1.92 | 45.2 | 27.96 | 0.07 |
| 3.65 | 44.51 | 1.61 | 50.2 | 27.42 | 0.21 |
| 4.15 | 44.11 | 1.73 | | | |

being listed in Table IV. All the uncertainties in Table IV are statistical in nature, and as usual are cited at the one standard deviation confidence level.

The behaviour of the positron total cross section, at low energies, is again consistent with what one might anticipate for a species possessing a relatively large permanent dipole moment and a dipole polarisability of some size. Namely, its magnitude increases significantly as you go to lower incident positron energies. The positron TCS of tetrahydropyran is also featureless, displaying only the characteristic changes in slope at the opening of the Ps and IP thresholds. The exception to this general statement might, however, be the small "hump" we observe at energies between ~5–7 eV. We believe this feature might be associated with the opening of discrete electronic-states in this energy regime. The electron–$C_5H_{10}O$ total cross section,[16] on the other hand, displays significant structure associated with the temporary capture of the incident electron by tetrahydropyran. It is a little surprising, at about 3 eV, that the electron TCS crosses that of the positron TCS and remains systematically lower in value at lower energies. This was not what we expected, as at these low energies electron exchange might be expected to be significant in the electron scattering case whereas in the positron case we are below the opening of the positronium formation channel. The data of Szmytkowski and Ptasińska-Denga[16] is not corrected for forward angle scattering effects, and so this observation might well be associated with forward scattering rather than indicating any particularly interesting physical phenomenon. Similar to what we observed in ethylene oxide, the trend in the positron–$C_5H_{10}O$ TCS converges to that of the electron TCS at an energy in the range 200–300 eV. Again we believe this makes good physical sense, as contributions from either positronium formation (positrons) or exchange (electrons) can be ignored at those higher energies.

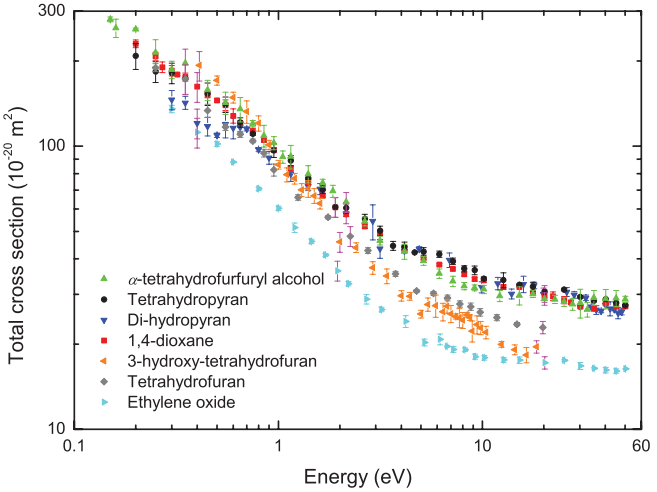


FIG. 5. TCSs ($\times 10^{-20}$ m$^2$) for positron scattering from the cyclic ethers, as studied previously[8–11] at the University of Trento and also as a part of this investigation. See legend on the figure for further details. Note that indicative total uncertainties, for each species, are plotted at selected energies in magenta in this figure.

### D. Comparative behaviour of the cyclic ethers

In Fig. 5 we plot all of our positron TCS scattering data that we have accumulated at the University of Trento over the last 8 (2004–2011) years for collisions with the cyclic ethers tetrahydropyran, α-tetrahydrofurfuryl alcohol, di-hydropyran, 1,4-dioxane, tetrahydrofuran, 3-hydroxy-tetrahydrofuran, and ethylene oxide. This figure should be considered in parallel with Table I, which contains a small selection of some of the important physico-chemical properties of these species. The most striking aspect of Fig. 5 is just how qualitatively similar is the energy dependence of the total cross section for each species in the energy range we have studied. While there are some differences due to the different positronium formation thresholds and first ionisation potentials between the various cyclic ethers, the similarity in the form of the various cross sections is quite remarkable. If we try and group these molecules in terms of the values of their dipole polarisabilities, then we see a natural division (see Table I) between those species with a relatively "high" value (di-hydropyran ($\alpha \sim 65$ a.u.), tetrahydropyran ($\alpha \sim 66$ a.u.), α-tetrahydrofurfuryl alcohol ($\alpha \sim 70$ a.u.), and 1,4-dioxane ($\alpha \sim 59$ a.u.) – Group 1), those species with a "moderate" value (tetrahydrofuran ($\alpha \sim 47$ a.u.) and 3-hydroxy-tetrahydrofuran ($\alpha \sim 51$ a.u.) – Group 2) and finally that species with a relatively "low" value (ethylene oxide ($\alpha \sim 30$ a.u.) – Group 3). Considering Group 1, then we find all these species also have very similar values for the dipole polarisability and when we go to Fig. 5 it is also apparent that, to within the total uncertainties on our measurements, their TCSs are also very similar in terms of their shapes and absolute magnitudes. This correspondence between α and the TCS

should not be regarded as too surprising, as the San Diego group has, for many species, clearly established a link (albeit an empirical one) between the value of their positron binding energies ($\varepsilon_b$) (Ref. 42) and the value of $\alpha$. Makochekanwa *et al.*,[38] in their study on the positronium formation cross sections of formic acid and water, also observed a link between those cross sections and the dipole polarisabilities of those species. In other words, the importance of the target dipolarisability on the scattering dynamics in positron scattering systems is well established. A similar case, except at the lowest energies where the effect of the larger dipole moment of an important conformer of 3-hydroxy-tetrahydrofuran plays an important role, can also be made for the Group 2 species. Finally, for ethylene oxide, we see that its dipole polarisability is roughly half that of the species in Group 1 and intriguingly its TCS, over much of the common energy range, is also roughly half that of the Group 1 molecules. This observation raises the possibility that, at least for the cyclic ethers, a "universal TCS function" might be constructed for those scientists seeking to model charged-particle tracks in that type of matter.[4,5]

## V. CONCLUSIONS

We have reported a comprehensive set of total cross sections for positron scattering from the cyclic ethers oxirane (ethylene oxide), 1,4-dioxane, and tetrahydropyran. We have also reported detailed elastic integral cross sections, as computed in the SMC formulation and at various levels of approximation for ethylene oxide. We believe all these data are unique, since we can find no evidence in the literature for any previous positron investigation of those molecules. The present results, particularly when combined with results from our earlier studies of some of the other cyclic ethers,[8–11] provide strong evidence in support of the view that the target dipole polarisability plays a very important role in the positron scattering dynamics for these systems.

A comparison, where possible, with corresponding electron total cross sections,[16–18] suggested that between 200–300 eV incident impact energy the magnitudes of the positron and electron TCSs were converging towards a common value. This makes good physical sense as two of the major processes that set positron and electron scattering apart, namely, positronium formation and exchange are expected to be negligible by 100 eV. Under these circumstances the scattering dynamics, at such high energies, are effectively impulsive, so that the charge on the incident projectile becomes unimportant.

## ACKNOWLEDGMENTS

This work was supported under a Memorandum of Understanding between the University of Trento and the Flinders University node of the ARC Centre of Excellence for Antimatter-Matter Studies. One of the authors (L.C.) would additionally like to thank CAMS for some financial support during his visit to Australia. M.H.F.B., S.d'A.S, M.T. do N.V., and M.A.P.L. acknowledge support from Brazilian agency Conselho Nacional de Desenvolvimento Científico e Tecnológico (CNPq). M.H.F.B. also acknowledges support from FINEP, while M.T. do N.V. and M.A.P.L. acknowledge the FAPESP. M.H.F.B. and S.d'A.S. thank Professor C. M. de Carvalho for computational support and all four Brazilian co-authors acknowledge additional computational support from CENAPAD–SP. We all thank Dr. L. Campbell for his assistance in the production of this paper and Professor S. J. Buckman for helpful comments.

[1] B. Boudaiffa, P. Cloutier, D. Hunting, M. A. Huels, and L. Sanche, Science **287**, 1658 (2000).
[2] A.-C. Hassan, P.-C. Dugal, and L. Sanche, Radiat. Res. **153**, 23 (2000).
[3] P. L. Levesque, M. Michaud, and L. Sanche, J. Chem. Phys. **122**, 094701 (2005).
[4] M. C. Fuss, A. Muñoz, J. C. Oller, F. Blanco, M.-J. Hubin-Franskin, D. Almeida, P. Limão-Vieira, and G. García, Chem. Phys. Lett. **486**, 110 (2010).
[5] A. Muñoz, F. Blanco, G. García, P. A. Thorn, M. J. Brunger, J. P. Sullivan, and S. J. Buckman, Int. J. Mass Spectrom. **277**, 175 (2008).
[6] I. Plante and F. A. Cucinotta, New J. Phys. **10**, 125020 (2008).
[7] R. D. White and R. E. Robson, Phys. Rev. Lett. **102**, 230602 (2009).
[8] A. Zecca, C. Perazzolli, and M. J. Brunger, J. Phys. B **38**, 2079 (2005).
[9] A. Zecca, L. Chiari, A. Sarkar, and M. J. Brunger, J. Phys. B **41**, 085201 (2008).
[10] A. Zecca, L. Chiari, K. L. Nixon, M. J. Brunger, S. Chattopadhyay, D. Sanyal, and M. Chakrabarti, J. Phys. Chem. A **113**, 14251 (2009).
[11] A. Zecca, L. Chiari, G. García, F. Blanco, E. Trainotti, and M. J. Brunger, New J. Phys. **13**, 063019 (2011).
[12] J. S. E. Germano and M. A. P. Lima, Phys. Rev. A **47**, 3976 (1993).
[13] E. P. da Silva, J. S. E. Germano, and M. A. P. Lima, Phys. Rev. A **49**, R1527 (1994).
[14] E. P. da Silva, J. S. E. Germano, J. L. S. Lino, C. R. C. de Carvalho, A. P. P. Natalense, and M. A. P. Lima, Nucl. Instrum. Methods Phys. Res. B **143**, 140 (1998).
[15] M. A. Khakoo, J. Blumer, K. Keane, C. Campbell, H. Silva, M. C. A. Lopes, C. Winstead, V. McKoy, R. F. da Costa, L. G. Ferreira, M. A. P. Lima, and M. H. F. Bettega, Phys. Rev. A **77**, 042705 (2008).
[16] C. Szmytkowski and E. Ptasińska-Denga, J. Phys. B **44**, 015203 (2011).
[17] C. Szmytkowski, A. Domaracka, P. Możejko, and E. Ptasińska-Denga, J. Chem. Phys. **130**, 134316 (2009).
[18] C. Szmytkowski, A. Domaracka, P. Możejko, and E. Ptasińska-Denga, J. Phys. B **41**, 065204 (2008).
[19] K. Watanabe, J. Chem. Phys. **26**, 542 (1957).
[20] *CRC Handbook of Chemistry and Physics*, 76th ed., edited by D. R. Lide (CRC, Boca Raton, Fl, 1995).
[21] D. A. Sweigart and D. W. Turner, J. Am. Chem. Soc. **94**, 5592 (1972).
[22] L. Jensen and P. T. van Duijnen, J. Chem. Phys. **123**, 074307 (2005).
[23] K. Watanabe, T. Nakayama, and J. Mottl, J. Quant. Spectrosc. Radiat. Transf. **2**, 369 (1962).
[24] V. M. Rao and R. Kewley, Can. J. Chem. **50**, 955 (1972).
[25] A. Zecca, L. Chiari, A. Sarkar, and M. J. Brunger, New J. Phys. **13**, 115001 (2011).
[26] A. Zecca, L. Chiari, A. Sarkar, S. Chattopadhyay, and M. J. Brunger, Nucl. Instrum. Methods Phys. Res. B **268**, 533 (2010).
[27] A. Zecca, L. Chiari, E. Trainotti, D. V. Fursa, I. Bray, A. Sarkar, S. Chattopadhyay, K. Ratnavelu, and M. J. Brunger, J. Phys. B **45**, 015203 (2012).
[28] A. Zecca, L. Chiari, E. Trainotti, D. V. Fursa, I. Bray, and M. J. Brunger, Eur. Phys. J. D **64**, 317 (2011).
[29] W. E. Kauppila, T. S. Stein, J. H. Smart, M. S. Dababneh, Y. K. Ho, J. P. Downing, and V. Pol, Phys. Rev. A **24**, 725 (1981).
[30] A. Hamada and O. Sueoka, J. Phys. B **27**, 5055 (1994).
[31] J. P. Sullivan, C. Makochekanwa, A. Jones, P. Caradonna, D. S. Slaughter, J. Machacek, R. P. McEachran, D. W. Mueller, and S. J. Buckman, J. Phys. B **44**, 035201 (2011).
[32] A. Zecca and M. J. Brunger, in *Nanoscale Interactions and their Applications: Essays in Hounour of Ian McCarthy*, edited by F. Wang and M. J. Brunger (Research Signpost, Trivandrum, India, 2007), p. 21.

[33]T. Takaishi and Y. Sensui, Trans. Faraday Soc. **59**, 2503 (1963).
[34]*CRC Handbook of Chemistry and Physics*, 79th ed., edited by D. R. Lide (CRC, Boca Raton, Fl, 1998).
[35]A. Zecca, E. Trainotti, L. Chiari, G. García, F. Blanco, M. H. F. Bettega, M. T. do N. Varella, M. A. P. Lima, and M. J. Brunger, J. Phys. B **44**, 195202 (2011).
[36]W. J. Hunt and W. A. Goddard III, Chem. Phys. Lett. **3**, 414 (1969).
[37]A. Zecca, L. Chiari, A. Sarkar, M. A. P. Lima, M. H. F. Bettega, K. L. Nixon, and M. J. Brunger, Phys. Rev. A **78**, 042707 (2008).
[38]C. Makochekanwa, A. Bankovic, W. Tattersall, A. Jones, P. Caradonna, D. S. Slaughter, K. Nixon, M. J. Brunger, Z. Petrovic, J. P. Sullivan, and S. J. Buckman, New J. Phys. **11**, 103036 (2009).
[39]A. Zecca, D. Sanyal, M. Chakrabarti, and M. J. Brunger, J. Phys. B **39**, 1597 (2006).
[40]A. Zecca, L. Chiari, E. Trainotti, A. Sarkar, and M. J. Brunger, PMC Phys. B **3**, 4 (2010).
[41]A. Zecca, L. Chiari, G. Garcia, F. Blanco, E. Trainotti, and M. J. Brunger, J. Phys. B **43**, 215204 (2010).
[42]G. F. Gribakin, J. A. Young, and C. M. Surko, Rev. Mod. Phys. **82**, 2557 (2010).